International Journal of Thermophysics, Vol. 20, No. 1, 1999

The Adsorption of Mixed Surfactants at the Hydrophilic Silica Surface from Aqueous Solution: Studied by Specular Neutron Reflection[1]

J. Penfold,[2,3] E. J. Staples,[2] I. Tucker,[4] L. J. Thompson,[4] and R. K. Thomas[5]

Specular neutron reflection has been used to determine the structure and composition of the mixed ionic–non-ionic surfactants adsorbed at the hydrophilic silica solid/water interface. Measurements on two different mixed surfactant systems are reported: the cationic/nonionic mixture of hexadecyltrimethyl ammonium bromide, $C_{16}TAB$, and hexaethylene glycol monododecyl ether, $C_{12}E_6$, and the anionic/nonionic mixture of sodium dodecyl sulfate, and $C_{12}E_6$. For the $C_{16}TAB$–$C_{12}E_6$ mixture, pH is shown to have a dramatic effect on the relative affinity for adsorption of the two surfactants at the interface.

KEY WORDS: adsorption; hydrophilic interface; mixed surfactants; neutron reflectivity.

1. INTRODUCTION

The study of mixed surfactant adsorption is of considerable interest because the mechanisms underlying the synergistic behavior frequently exploited in commercial applications of surfactant mixtures are not well understood. The adsorption of surfactants, and particularly mixed surfactants, is important in a wide range of technological and industrial applications, which

[1] Invited paper presented at the Thirteenth Symposium on Thermophysical Properties, June 22–27, 1997, Boulder, Colorado, U.S.A.

[2] ISIS Facility, CLRC, Rutherford Appleton Laboratory, Chilton, Didcot, Oxon OX11 OQX, United Kingdom.

[3] To whom correspondence should be addressed.

[4] Unilever Research, Port Sunlight Laboratory, Quarry Road East, Bebington, Wirral, United Kingdom.

[5] Physical and Theoretical Chemistry, Oxford University, South Parks Road, Oxford, United Kingdom.

0195-928X/99/0100-0019$16.00/0

include detergency, fabric conditioning, dyeing, mineral flotation, colloidal stability, and surface modification.

Recently, specular neutron reflection has emerged as a powerful technique for the study of surfactant adsorption at the air/water interface [1]. Isotopic labeling, through H/D isotopic substitution, enables the structure and adsorbed amount to be determined [2–4]. For mixtures, particularly, this allows both the surface composition and the structure [5–9] to be determined. It provides a selectivity not available in techniques such as ellipsometry [10] and x-ray reflectivity [11], and information complementary to the optical techniques of sum frequency and second harmonic generation [12]. In the study of surfactant adsorption at the liquid–solid interface, techniques such as fluorescence decay [13], solution depletion [14], ellipsometry [10], x-ray reflectivity [11], and atomic force microscopy [15] provide either little or no structural information, or do not have the selectivity required to study mixtures. Brinck and Tiberg [16] have used ellipsometry to provide indirectly information about the adsorption of mixed nonionic surfactants at the silica–water interface, where the total adsorbed amounts at different solution compositions have been measured. The ellipsometric measurements, in particular, offer the opportunity to obtain kinetic as well as equilibrium information. More recently, Thomas and coworkers [17–21] have demonstrated that specular neutron reflection can provide detailed information on the adsorption of surfactants at the liquid–solid interface and the structure of nonionic surfactants [17, 18, 20] and cationic surfactants [19, 21] have been determined at both the hydrophilic and the hydrophobic solid interfaces. In contrast there have to date been only limited investigations of surfactant mixtures adsorbed at the liquid/solid interface [22].

The adsorption of nonionic surfactants at the hydrophilic silica interface is known to be strongly pH dependent [17]: for pH values $\geqslant 9.0$ the nonionic surfactants desorb, whereas at low pH (<4.0) they always strongly adsorb. The adsorption is due to hydrogen bonding between the ether oxygens of the nonionic surfactants and hydroxyl groups on the silica surface and, so, is dependent upon the density of hydroxyl groups on the surface. In the past this has caused some variability in nonionic adsorption onto hydrophilic silica, due to variations in surface treatment and, hence, in the density of hydroxyl groups on the surface. We have exploited this in the work described in this paper to investigate the relationship between this hydrogen bonding and the specific interaction of the surfactant with the surface, the structure, and composition of mixed surfactants adsorbed at the liquid–solid interface. In this paper we contrast the results from two different surfactant mixtures. The cationic–nonionic and anionic–nonionic surfactant mixtures studied are mixtures whose adsorption behavior at the

air–water interface have previously been studied by neutron reflectivity [6, 8, 9]. In the cationic/nonionic mixture of $C_{16}TAB/C_{12}E_6$, the affinity of the $C_{12}E_6$ for the interface is manipulated by pH. In the anionic/nonionic surfactant mixture of sodium dodecyl sulfate (SDS)/$C_{12}E_6$, the SDS is present only at the interface due to the adsorption of the $C_{12}E_6$, that is, the need to maintain equilibrium between the bulk solution and the interface. SDS alone does not adsorb to the hydrophilic silica surface.

We have used specular neutron reflection to determine the structure and the composition of the mixed surfactants at the hydrophilic silica-water interface. Measurements were made for an equimolar mixture of $C_{16}TAB$ and $C_{12}E_6$ at pH values of 7.0 and 2.4, and for 70 mol% $C_{16}TAB$/30 mol% $C_{12}E_6$ and 30 mol% $C_{16}TAB$/70 mol% $C_{12}E_6$ at a pH of 2.4. All the measurements for $C_{16}TAB/C_{12}E_6$ were made in the presence of 0.1 *M* NaBr, and at a surfactant concentration of 10^{-4} *M*. Measurements for the SDS/$C_{12}E_6$ mixture were made at a pH of 7.0, at a surfactant concentration of 2.5×10^{-3} *M*, in 0.1 *M* NaBr, for a solution composition of 70 mol% SDS/30 mol% $C_{12}E_6$. The measurements were all made at concentrations higher than the critical micellar concentrations (CMC) for the mixtures, in a region where saturation adsorption is achieved. A series of different neutron reflectivity measurements was made with different isotopically labeled combinations of surfactant and solvent. The resulting reflectivity profiles were analyzed using models calculated for the exact optical matrix formulation [23, 24].

2. NEUTRON REFLECTIVITY

Specular neutron reflection gives information about inhomogeneities normal to an interface or surface, and its theory has been described in detail elsewhere [1]. The basis of a neutron reflection measurement is that the variation in specular reflection with κ (the wave vector transfer defined as $\kappa = 4\pi \sin\theta/\lambda$, where θ is the glancing angle of incidence, and λ the neutron wavelength) is simply related to the composition or concentration profile in the direction normal to the interface. In the kinematic approximation [25] the specular reflectivity, $R(\kappa)$, is given by

$$R(\kappa) = \frac{16\pi^2}{\kappa^2} |\rho(\kappa)|^2 \tag{1}$$

where $\rho(\kappa)$ is the one-dimensional Fourier transform of $\rho(z)$, the average scattering length density profile in the direction normal to the interface,

$$\rho(\kappa) = \int_{-\infty}^{\infty} \rho(z) \exp(i\kappa z)\, dz \tag{2}$$

and,

$$\rho(z) = \sum_i n_i(z)\, b_i \tag{3}$$

where n_i is the number density profile of species i and b_i is its scattering length. In the context of surfactant adsorption, the key feature of the neutron reflectivity method is that the neutron scattering properties of H and D are sufficiently different that, for studying adsorption at both the air–liquid and the liquid–solid interfaces, H/D isotopic substitution can be used to manipulate the neutron refractive index profile at that interface. This is particularly important for surfactant mixtures, where, by selective deuteration, particular components or fragments can be highlighted. It is this selectivity which makes the neutron reflectivity method so powerful. The effectiveness of the method in determining the surfactant structure depends on being able to combine reflectivity profiles from solutions of the same chemical but different isotopic composition. This, of course, assumes that there is no isotopic dependence of the structure on adsorbed amounts, and this is now being established [26].

In terms of structure, the reflectivity profiles can be analyzed by, principally, two methods. In the first method, a structural model is assumed for the interface, and the reflectivity calculated exactly using the optical matrix method [23, 24]. The model is then optimized to fit simultaneously the reflectivity profiles for the different isotopically labeled combinations. Alternatively a more direct method, based on the kinematic approximation [3], is used to analyze the reflectivity profiles from the different isotopic combinations by separating out the contributions from the different components of the interfacial layer. The latter approach has now been extensively applied to the determination of the structure of the adsorbed surfactant layer at the air–water interface and has, for example, been used to determine the structure of the C_{16}TAB monolayer at the air–water interface to a resolution of two methylene groups [4]. For the study of adsorption at the liquid–solid interface, where the structure is more complicated and it is difficult to isolate the contribution from all the individual components, the former approach based on model fitting (using a least-squares criterion) and the optical matrix methods of calculation provide, in practice, the only satisfactory route to analyze the data.

3. EXPERIMENTAL

The specular neutron reflection measurements were made on the SURF reflectometer [27] at the ISIS pulsed neutron source, using the "white"

beam time-of-flight method. Measurements were made in the κ range of 0.012 to 0.4 $Å^{-1}$ using a wavelength band of 1 to 7.0 Å and three glancing angles of incidence, 0.35, 0.8, and 1.8°. The sample geometry, now well established for liquid–solid studies, is used, that is, the neutron beam is incident at glancing angles at the liquid–solid interface by transmission through the crystalline silicon upper phase. The sample cell has been described previously and was developed originally for Poiseuille shear flow measurements at grazing incidence [28] but is used here for static measurements. The polished silicon single ($\langle 111 \rangle$ face) crystal was obtained from Semiconductor Processing (Boston) and was used without any additional surface treatment. The illuminated area was 30×60 mm, and the resolution in κ, $\Delta\kappa/\kappa$ was $\sim 4\%$. The data were normalized for the incident beam spectral distribution, detector efficiency, and silicon transmission using standard procedures and established on an absolute reflectivity scale by reference to the direct beam intensity.

Reflectivity measurements were made for the mixture of $C_{16}TAB/C_{12}E_6$ in 0.1 *M* NaCl at a concentration of 10^{-4} *M* and at two pH values, 2.4 and 7.0 (adjusted by the addition of HCl). Measurements were made for the equimolar mixture of $C_{16}TAB/C_{12}E_6$ at pH values of 2.4 and 7.0, and of

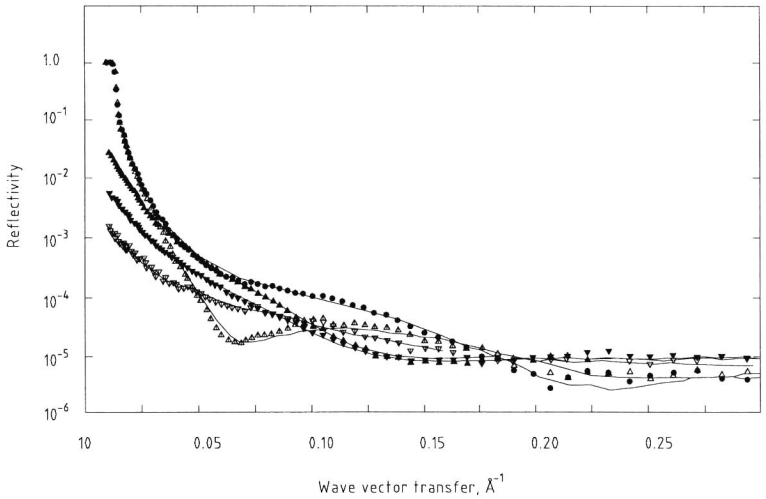

Fig. 1. Neutron reflectivity profiles for the equimolar mixture $C_{16}TAB/C_{12}E_6$ at 10^{-4} *M* in 0.1 *M* NaBr at the Si/SiO_2 interface for (●) $dC_{16}dTAB/hC_{12}hE_6$ in D_20 (△) $hC_{16}dTAB/dC_{12}hE_6$ in D_2O, (▲) $dC_{16}dTAB/dC_{12}hE_6$ in H_2O, (▼) $dC_{16}dTAB/hC_{12}hE_6$ in H_2O, and (△) $hC_{16}dTAB/dC_{12}hE_6$ in H_2O: the solid lines are profiles calculated for the bilayer model described in the text, with parameters given in Table I.

the mixtures 30 mol% C_{16}TAB/70 mol% $C_{12}E_6$ and 70 mol% C_{16}TAB/30 mol% $C_{12}E_6$ at a pH of 2.4. Measurements were made for hC_{16}hTAB/$hC_{12}hE_6$, dC_{16}dTAB/$hC_{12}hE_6$, and hC_{16}hTAB/$dC_{12}hE_6$ in D_2O, dC_{16}dTAB/$dC_{12}hE_6$, dC_{16}dTAB/$hC_{12}hE_6$, and hC_{16}hTAB/$dC_{12}hE_6$ in H_2O, dC_{16}dTAB/$hC_{12}hE_6$ in D_2O, and CMS_i at pH 7.0. The SDS/$C_{12}E_6$ mixture was measured at a surfactant concentration of 2.5×10^{-3} *M* and 0.1 *M* NaBr and for a solution composition of 70 mol% SDS/30 mol% $C_{12}E_6$. The measurements were made using the isotopic combinations of h-SDS/$dC_{12}E_6$ in H_2O and D_2O, d-SDS/$hC_{12}hE_6$ in H_2O and D_2O, and d-SDS/$hC_{12}hE_6$ in H_2O. All the measurements were made at a temperature of 30°C, unless otherwise stated and in 0.1 *M* NaBr.

The $hC_{12}hE_6$ was obtained from Fluka and purified by chromatography [26], and the other isotopes of $C_{12}E_6$, C_{16}TAB, and SDS were synthesized by R. K. Thomas at Oxford. The details of the preparation, purification, and characterization are given elsewhere [25, 26]. High-purity water was used for all the measurements (Elga Ultrapure), and the D_2O was obtained from Flourochem. All glassware and the sample cell were cleaned using alkaline detergent (Decon 90), followed by copious washing in ultrapure water, rinsing to non-foaming end points.

The contribution to the reflectivity at the silicon–solution interface from the thin oxide layer on the silicon surface is not negligible and must be included in any model calculations. It is hence important to characterize the nature of that oxide layer at the silicon surface. This is done by making measurements (in the absence of surfactant) of the silicon–water interface with different water contrasts (normally D_2O, H_2O, and water index-matched to silicon, cmSi). These measurements have been previously made for the two sides of the silicon block used in these measurements [29]. The thickness of the oxide layer was, within error, the same on each side (20 ± 2 Å), but the composition of the two oxide layers was slightly different. The variation of scattering length density with solvent contrast, from the single model fits used to obtain the oxide layer thickness, are consistent with a solvated layer. The volume fractions of solvent were 24 and 32% for the two sides of the block, respectively. These parameters describing the oxide layer are consistent with other recent measurements [20, 21] and are typical of the oxide layer that forms on the $\langle 111 \rangle$ face of silicon. Prior to the measurements of the adsorption of the surfactant mixtures, the adsorption of $C_{12}E_6$ and C_{16}TAB alone was measured. The measurements were made for different surfactant and solvent isotopic labeling. The C_{16}TAB was measured at a pH of 7.0 and the $C_{12}E_6$ at pH values of 2.4 and 7.0. The details of this characterization are described in detail elsewhere [29] and will not be repeated, as the emphasis here is on the adsorption of the mixtures.

It has been well established by reflectivity measurements and SANS measurements [30, 31] in nonionic surfactant adsorption and reflectivity measurements on cationic surfactants [19] that the nature of the adsorbed layer is a fragmented bilayer. The adsorbed layer can then be described by three layers: a layer of thickness d_1 adjacent to the solid surface containing headgroups and the associated hydration, a layer of thickness d_2 containing the hydrocarbon chains interpenetrating (or overlapping) from both sides of the bilayer, and a layer of thickness d_3 adjacent to the fluid phase containing headgroups and hydration. In many cases, where the structure of the bilayer is not sufficiently well ordered, an additional parameter, f_c is required, which allows for some intermixing between the headgroup and alkyl chain regions. f_c is then the fraction of alkyl chains in the headgroup region. The model can then be described by three thicknesses, d_1, d_2 and d_3, the area per molecule in the bilayer, A, f_c, and the fractional coverage, f (the fraction of the surface covered by bilayer patches). From the known molecular volumes and scattering lengths, the scattering length densities of each of the layers can be estimated. This is also the basis of the model used to analyze the reflectivity data for the surfactant mixtures. The results obtained from modeling the reflectivity for $C_{12}E_6$ and $C_{16}TAB$ (at a concentration of 10^{-4} M in 0.1 M NaBr where saturation adsorption is achieved) [17] are consistent with other measurements [17–21]. For $C_{16}TAB$ the coverage was 0.73 ± 0.04 and independent of pH. In contrast, the adsorption of the $C_{12}E_6$ is strongly pH dependent and, in these measurements, gave a coverage of 0.12 ± 0.04 at pH 7.0 and 0.5 ± 0.02 at pH 2.4.

4. RESULTS AND DISCUSSION

Figure 1 shows the specular reflectivity profiles for the adsorption at the Si/SiO_2 interface from an equimolar mixture of $C_{16}TAB/C_{12}E_6$ at 10^{-4} M in 0.1 M NaBr and at a pH of 2.4. The profiles in Fig. 1 are for the differently labeled surfactant combinations in D_2O and H_2O.

The simplest model that is consistent with all the data is a fragmented interdigittated bilayer, similar to that used for $C_{12}E_6$ alone. The parameters in Table I give an indication of the spread in values from the fits to the different isotopically-labelled combinations. The procedure adopted was to refine the individual model parameters [d_1, d_2, d_3, f_d (see later discussion), f, f_c, A_c, A_n] for each profile using a least-squares criterion to give the minimal spread in the model parameters for all the contrasts measured. Figure 1 shows the specular reflectivity profiles for the adsorption at the

Table I. Parameters Used to Fit $C_{16}TAB/C_{12}E_6$ Bilayer Adsorbed at the Si/SiO_2 Solution (as Described in the Text)

Contrast	pH	d_1	d_2	d_3	f_d[a]	f	f_c	A_c[a]	A_n[a]
$hC_{16}hTAB/hC_{12}hE_6/D_2O$	2.4	14.7	13.6	10.8	1.0	0.78	0.2	57.5	63.3
$dC_{16}dTAB/hC_{12}hE_6/D_2O$	2.4	13.9	14.4	11.1	"	0.95	"	61.3	60.2
$hC_{16}hTAB/dC_{12}hE_6/D_2O$	2.4	11.8	13.9	7.4	"	0.87	"	59.8	71.5
$dC_{16}dTAB/dC_{12}hE_6/H_2O$	2.4	14.1	11.4	14.0	"	0.74	"	58.1	53.3
$dC_{16}dTAB/hC_{12}hE_6/H_2O$	2.4	14.2	14.8	15.8	"	0.77	"	49.7	48.5
$hC_{16}dTAB/dC_{12}hE_6/H_2O$	2.4	13.9	12.8	14.0	"	0.75	"	53.4	58.6
$hC_{16}hTAB/hC_{12}hE_6/D_2O$	7.0	7.4	11.4	10.6	0.85	0.86	0.11	41.4	83.2
$dC_{16}dTAB/hC_{12}hE_6/D_2O$	7.0	6.8	11.8	6.3	0.53	1.0	0.09	39.4	104.0
$dC_{16}hTAB/hC_{12}hE_6/H_2O$	7.0	7.5	16.5	15.7	0.97	0.78	0.10	37.1	78.1
$hC_{16}dTAB/hC_{12}hE_6/CmSi$	7.0	6.1	13.7	15.3	0.88	0.83	0.10	33.9	82.0
$dC_{16}dTAB/hC_{12}hE_6/CmSi$	7.0	9.3	15.1	12.9	0.89	0.78	0.05	39.8	112.0

[a] A_c and A_n are the areas/molecule of the $C_{16}TAB$ and $C_{12}E_6$, and f_d is a weighting factor which describes any asymmetry in the composition within the bilayer (see text for detailed explanation).

Si/SiO_2 interface from an equimolar mixture on $C_{16}TAB/C_{12}E_6$ at 10^{-4} *M* in 0.1 *M* NaBr and at a pH of 2.4.

From the analysis of the data in Fig. 1, the labeled combination of $dC_{16}dTAB/hC_{12}hE_6$ in D_2O provides a good estimate of the amount of $C_{12}E_6$ adsorbed at the interface. The greater the deviation of the reflectivity profile from that measured for the $Si/SiO_2/D_2O$ interface alone, the greater is the amount of $C_{12}E_6$ in the adsorbed layer. The marked difference between the two profiles measured at pH 7.0 and 2.4 is indicative of an increase in the amount of $C_{12}E_6$ adsorbed with decreasing pH (see Fig. 2). This is borne out by the subsequent more detailed analysis.

The main structural features are that at pH 2.4 the bilayer is essentially symmetrical; the two headgroup regions are, within experimental error, identical and the alkyl chain region is less than the dimension of a fully extended chain. This is due, in part, to the fraction of chains in the headgroup region, f_c, ~ 0.2, which stems primarily from constraints arising from the disparity in headgroup size between the $C_{16}TAB$ and $C_{12}E_6$. At pH 7.0 the structure of the bilayer is not symmetrical; although the alkyl chain region and headgroup layer adjacent to the solvent are of dimensions similar to those at pH 2.4, the headgroup region adjacent to the solid phase (Si/SiO_2) is significantly thinner (7.4 Å compared to 13.8 Å). This asymmetry results from the two surfactants being unevenly distributed across the bilayer at the higher value of pH. The layer adjacent to the solid phase has a higher mole fraction of cationic surfactant than the outer layer. An

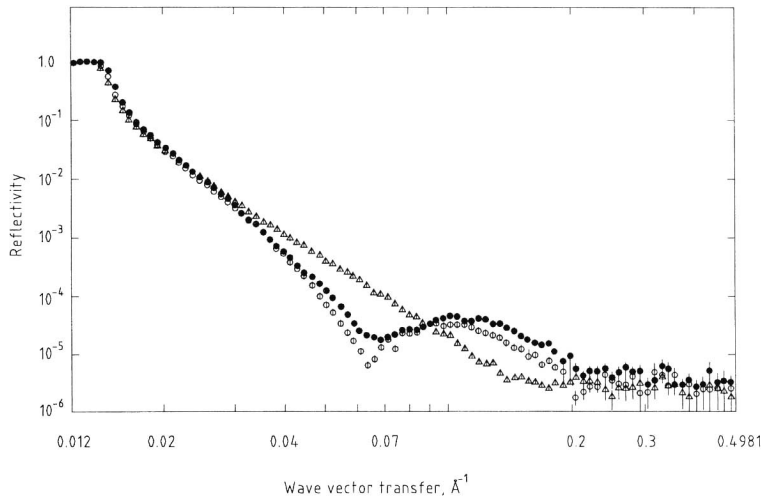

Fig. 2. Neutron reflectivity profiles for a 10^{-4} *M* equimolar mixture of $C_{16}TAB/C_{12}E_6$ in 0.1 *M* NaBr at the Si/SiO_2 interface, (●) $dC_{16}dTAB/hC_{12}hE_6$ in D_2O at pH 2.4, and (○) at pH 7.0 and (△) in D_2O only (no surfactant).

additional model parameter, f_d, has been introduced to accommodate this asymmetry in distribution, and f_d is a weighting factor which describes that asymmetry in distribution across the bilayer. At pH 2.4, f_d is unity, and the surfactant composition is the same in both halves of the bilayer, whereas at pH 7.0, $f_d \sim 0.82$, indicating that there is $\sim 20\%$ more cationic surfactant than nonionic surfactant in the layer adjacent to the solid phase and consequently the outer layer is richer in nonionic surfactant. The reduction in pH from 7.0 to 2.4 reduces the charge density on the silica surface and, at pH 2.4, is close to the zero point of charge [32]. This means that at low pH the adsorption mechanism is dominated by the $C_{12}E_6$ and the $C_{16}TAB$ is present due to the entropy of mixing. At high pH the $C_{16}TAB$ has a strong affinity for the surface, while the presence of surface charge reduces the possibility of hydrogen bonding for the $C_{12}E_6$.

The fractional coverage of the fragmented bilayer is similar at both values of pH and is close to the maximum value observed for $C_{12}E_6$ and $C_{16}TAB$ alone [17–22]. At pH 2.4 the total adsorbed amount is slightly less than that at pH 7.0, but in both cases the amount adsorbed is significantly larger than obtained for single surfactants. At pH 7.0, where the affinity of the $C_{12}E_6$ for the surface is significantly reduced, the surface composition is rich in $C_{16}TAB$ (mol% of $C_{16}TAB$ at the interface is ~ 70), whereas at pH 2.4, when the affinity of the $C_{12}E_6$ for the surface is greatly

enhanced, the surface composition is close to the bulk solution composition (mol% of $C_{16}TAB$, ~ 50).

Measurements were also made for different solution compositions, 30 mol% $C_{16}TAB$/70 mol% $C_{12}E_6$ and 70 mol% $C_{16}TAB$/30 mol% $C_{16}TAB$ at a pH of 2.4. These data were analyzed using the same model described for the equimoler mixtures. The mean value from the analysis of each labeled combination for all the $C_{16}TAB/C_{12}E_6$ data and their associated errors are summarized in Table II. The reflectivity data for the three labeled combinations in D_2O ($hC_{16}hTAB/hC_{12}hE_6$, $dC_{16}dTAB/hC_{12}hE_6$, and $hC_{16}hTAB/dC_{12}hE_6$) for the three solution compositions clearly show the changes in surface composition (see Fig. 3). For the 70/30 mixture the surface is close to the solution composition, and the mol% of $C_{16}TAB$ at the interface is 0.73. For the 30/70 mixture the surface is rich in $C_{16}TAB$ compared to the solution; the surface has 0.47 mol% of $C_{16}TAB$.

McDermott et al. [22] have used specular neutron reflection to study the adsorption of $C_{16}TAB/C_{12}E_6$ mixed surfactant at the crystalline–quartz interface in the absence of electrolyte. Measurements were made at concentrations $\geqslant$CMC of the mixture and for solution compositions with mole fractions of $C_{16}TAB$ of 0.55 and 0.92. Surface compositions, corresponding to $C_{16}TAB$ mole fractions of 0.05 and 0.77, were obtained for measurements with limited isotopically labeled combination. From regular solution theory (using an interaction parameter, $\beta \sim -2.1$, calculated from the CMC values) [33], the predicted micelle compositions were 0.26 and 0.78 mole fraction of $C_{16}TAB$. However, it is difficult to make a detailed comparison with our results because the measurements of McDermott et al. [22] were made in the absence of electrolyte and at a different solid interface.

Measurements of the composition at the air–liquid interface by neutron reflectometry (8) and of the micelle composition by SANS (8) have shown that the $C_{16}TAB/C_{12}E_6$ mixed surfactants exhibit essentially ideal mixing. At concentrations $\gg$CMC, the micelle and surface compositions should reflect the bulk composition, and this is found for many of the systems investigated [5–7] including the mixed surfactant $C_{16}TAB/C_{12}E_6$ [8]. For nonideal mixing, and even for ideal mixing, if the CMC of the two components are sufficiently different, the surface and micelle compositions can vary markedly in the region of the CMC, consistent with the predictions of regular solution theory [33]. For the $C_{16}TAB/C_{12}E_6$ mixture at 10^{-4} *M* and in 0.1 *M* NaBr, the surface composition at the air–solution interface is 60 mol% $C_{12}TAB$/40 mol% $C_{12}E_6$ (the CMC of the mixture is $\sim 6 \times 10^{-5}$ *M*), and at 3×10^{-4} *M* it is 54 mol% $C_{16}TAB$, close to the bulk composition. The compositions measured here for the adsorption at the hydrophilic Si/SiO_2 solid interface from equimolar $C_{16}TAB/C_{12}E_6$ at pH 7.0 and 2.4 are significantly different and evidence of the role of specific

Table II. Mean Values of Parameters from Model Fits to $C_{16}TAB/C_{12}E_6$ and $SDS/C_{12}E_6$ Mixtures

Solution	pH	d_1	d_2	d_3	f_d	f	f_c	A_1	A_2	Γ ($\times 10^{-10}$ mol · cm^{-1})	Mol% of component 1
50/50 $C_{16}TAB/C_{12}E_6$	2.4	13.8 ± 1	13.6 ± 1	12.2 ± 2	1.0	0.81 ± 0.08	0.2 ± 0.05	56.6 ± 4	59.2 ± 7	9.29 ± 0.10	0.51 ± 0.05
	7.0	7.4 ± 1	13.7 ± 2	12.2 ± 3.5	0.82 ± 0.15	0.85 ± 0.08	0.09 ± 0.02	38.3 ± 2.6	91.9 ± 13.5	10.44 ± 0.10	0.71 ± 0.05
70/30 $C_{16}TAB/C12E_6$	2.4	11.8 ± 0.6	11.9 ± 1.6	16.1 ± 2.1	0.94 ± 0.08	0.78 ± 0.06	0.24 ± 0.02	41 ± 3	108.0 ± 6	8.85 ± 0.1	0.73 ± 0.05
30/70 $C_{16}TAB/C_{12}E_6$	2.4	12.0 ± 1.4	10.9 ± 1.5	18.7 ± 1.5	0.95 ± 0.04	0.74 ± 0.06	0.22 ± 0.4	76 ± 7	67 ± 6	6.89 ± 0.1	0.47 ± 0.05
30/70 $SDS/C_{12}E_6$	7.0	13.7 ± 2	17.2 ± 3	17.3 ± 3	0.58 ± 0.04	0.21 ± 0.04	0.26/0.05 ± 0.02[a]	36.4 ± 4	91 ± 12	2.69 ± 0.1	0.71 ± 0.05

[a] Note that the $SDS/C_{12}E_6$ data could be analyzed only by assuming that the fractions of SDS and $C_{12}E_6$ chains in the headgroup region are different.

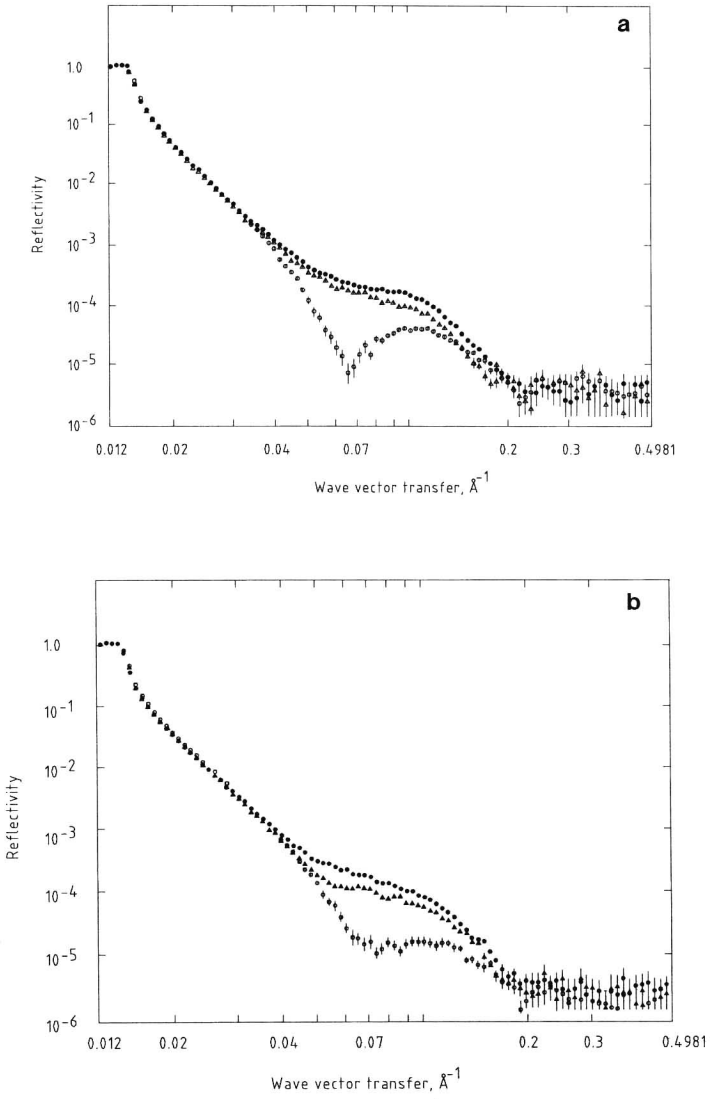

Fig. 3. Neutron reflectivity profiles for the mixed surfactants $C_{16}TAB/C_{12}E_6$ at 10^{-4} *M* in 0.1 *M* $NaBr/D_2O$ at the Si/SiO_2 interface for (a) an equimolar mixture, (b) 70 mol% $C_{16}TAB$, and (c) 30 mol% $C_{16}TAB$ (labeled combinations as in Fig. 1).

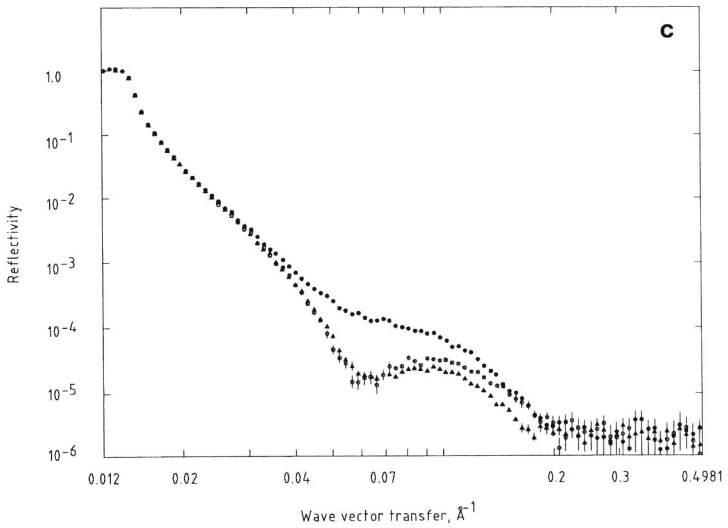

Fig. 3. *(Continued)*

surface interaction with the surfactants in determining the surface composition. In particular, the change in pH dramatically alters the surface composition, the decrease in pH resulting in a surface more rich in the nonionic surfactant. The surface compositions measured at different solution compositions at pH 2.4 are further evidence of the specific interaction with the surface. For the 70 mol% $C_{16}TAB$/30 mol% $C_{12}E_6$ mixture, the surface composition is close to that of the solution, whereas for the 30 mol% $C_{16}TAB$/70 mol% $C_{16}TAB$ mixture the surface is rich in $C_{16}TAB$.

For comparison with the $C_{16}TAB/C_{12}E_6$ mixtures, we have made some preliminary measurements on the $SDS/C_{12}E_6$ mixture, where the nature of the interaction with the surface is more extreme, in that the SDS, in the absence of $C_{12}E_6$, does not adsorb at the hydrophilic silica surface. The reflectivity data for 30 mol% SDS/70 mol% $C_{12}E_6$ in 0.1 *M* NaBr and at a surfactant concentration of 2.5×10^{-5} *M* is shown in Fig. 4.

The solid lines shown in Fig. 4 are model calculations using a model similar to that used for the $C_{16}TAB/C_{12}E_6$, and the mean parameters obtained from the fits to the reflectivity profiles for the differently labeled combinations are summarized in Table II. There are a number of important differences compared to the $C_{16}TAB/C_{12}E_6$ mixtures. For the $SDS/C_{12}E_6$ mixture the adsorbed amount is much less than that for $C_{16}TAB/C_{12}E_6$, reflecting the low affinity of the SDS for the surface and the $C_{12}E_6$ at a pH of 7.0. However, the surface composition is surprisingly heavily weighted

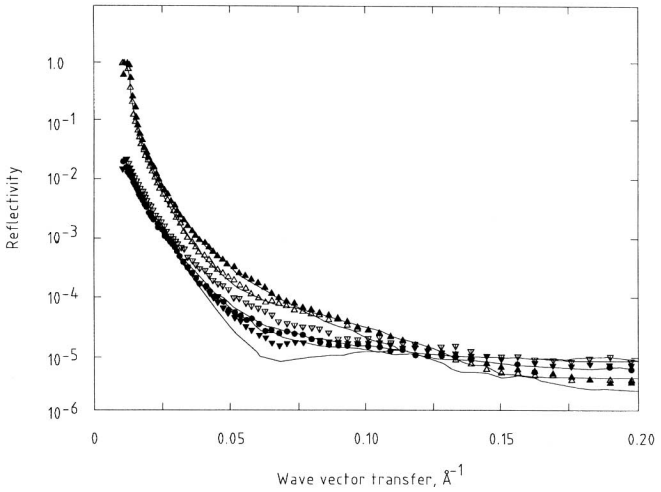

Fig. 4. Neutron reflectivity profiles for 2.5×10^{-3} *M* 70 mol% SDS/30 mol% $C_{12}E_6$ in 0.1 *M* NaBr for (▲) h-SDS/$dC_{12}hE_6$ in D_2O, (△) d-SDS/$hC_{12}hE_6$ in D_2O, (▼) d-SDS/$dC_{12}hE_6$ in H_2O, (▽) d-SDS/$hC_{12}hE_6$ in H_2O, and (●) h-SDS/$dC_{12}hE_6$ in H_2O. The solid lines are profiles calculated for a bilayer model described in the text, with the parameters given in Table II.

toward the SDS; the surface has ~ 70 mol% SDS in the adsorbed bilayer. The lack of affinity of the SDS for the hydrophilic surface, however, has a profound effect upon the structure of the adsorbed bilayer. In particular, the composition of the bilayer is now extremely asymmetric and the layer adjacent to the silica surface is 40% more nonionic than SDS. This asymmetry also has another effect on the structure of the bilayer in that the alkyl chain/headgroup mixing is different for the two surfactants, that is, there is more intermixing for the SDS than that for the $C_{12}E_6$. This is not seen in the $C_{16}TAB/C_{12}E_6$ mixtures.

5. SUMMARY

The structure and composition of the mixed surfactants of $C_{16}TAB/C_{12}E_6$ and of SDS/$C_{12}E_6$ adsorbed at the hydrophilic silica solid–solution interface have been determined by specular neutron reflectivity. The structure and composition of the bilayer formed at the interface are found to be profoundly affected by the relative affinity of the two surfactants for the surface. For the $C_{16}TAB/C_{12}E_6$ mixture, this is achieved by changing the pH of the solution from 7.0 to 2.4, where the affinity of the $C_{12}E_6$ for

the surface is substantially increased. This is contrasted with the SDS/$C_{12}E_6$ mixture, where the SDS does not adsorb at the hydrophilic surface in the absence of the cosurfactant. For the most part the surface compositions are significantly different from the bulk composition, the composition at the air–water interface, and the micellar composition, as previously obtained from neutron reflectivity and small-angle neutron scattering measurements [6]. The application of current theories, such as regular solution theory [33], would not predict such changes and will require modification to take into account the specific interaction of the surfactants with the solid surface, which clearly dominates the surface properties of the mixtures at the solid interface.

REFERENCES

1. J. Penfold and R. K. Thomas, *J. Phys. Condens. Matter* **2**:1369 (1990).
2. E. A. Simister, R. K. Thomas, J. Penfold, R. Aveyard, B. P. Binks, P. D. I. Fletcher, J. R. Lu, and A. Sokolowski, *J. Phys. Chem* **96**:1383 (1992).
3. E. A. Simister, E. M. Lee, R. K. Thomas, and J. Penfold, *J. Phys. Chem* **96**:1373 (1992).
4. J. R. Lu, Z. X. Li, J. Smallwood, R. K. Thomas, and J. Penfold, *J. Phys. Chem.* **99**:8233 (1995).
5. E. J. Staples, L. Thompson, I. Tucker, J. Penfold, R. K. Thomas, and J. R. Lu, *Langmuir* **9**:1651 (1993).
6. J. Penfold, E. Staples, I. Thompson, I. Tucker, J. Hines, R. K. Thomas, and J. R. Lu, *Langmuir* **11**:2496 (1995).
7. J. Penfold, E. Staples, L. Thompson, and I. Tucker, *Colloids and Surfaces* **102**:127 (1995).
8. J. Penfold, E. Staples, P. Cummins, I. Tucker, L. Thompson, R. K. Thomas, E. A. Simister, and J. R. Lu, *J. Chem. Soc. Faraday Trans.* **92**:1773 (1996).
9. J. Penfold, E. Staples, P. Cummins, I. Tucker, R. K. Thomas, E. A. Simister, and J. R. Lu, *J. Chem. Soc. Faraday Trans.* **92**:1547 (1996).
10. F. Tiberg, *J. Chem. Soc. Faraday Trans.* **92**:531 (1996).
11. T. P. Russell, *Mater. Sci. Dep.* **5**:171 (1990).
12. C. D. Bain, P. B. Davies, and R. N. Ward, *Langmuir* **10**:2000 (1994).
13. P. Levitz and H. Van Damne, *J. Phys. Chem.* **90**:1302 (1986).
14. H. B. Hough and H. M. Rendell, in *Adsorption from Solution at the Liquid/Solid Interface*, G. D. Parfitt and G. H. Rochester, eds. (Academic Press, London, 1983).
15. S. Mawie, J. P. Cleveland, H. E. Gamb, G. D. Stucky, and P. K. Honsma, *Langmuir* **10**:4409 (1994).
16. J. Brinck and F. Tiberg, *Langmuir* **12**:5042 (1996).
17. E. M. Lee, R. K. Thomas, P. G. Cummins, E. J. Staples, J. Penfold, and A. R. Rennie, *Chem. Phys. Lett.* **162**:196 (1989).
18. D. C. McDermott, J. R. Lu, E. M. Lee, R. K. Thomas, and A. R. Rennie, *Langmuir* **8**:204 (1992).
19. D. C. McDermott, J. McCarney, R. K. Thomas, and A. R. Rennie, *J. Coll. Int. Sci.* **162**:304 (1994).
20. G. Fragnetto, J. R. Lu, P. C. McDermott, R. K. Thomas, A. R. Rennie, P. D. Gallagher, and S. K. Satija, *Langmuir* **12**:477 (1996).

21. G. Fragnetto, R. K. Thomas, A. R. Rennie, and J. Penfold, *Langmuir* **12**:6036 (1996).
22. D. C. McDermott, D. Kanelleas, R. K. Thomas, A. R. Rennie, S. K. Satija, and L. F. Majkrzak, *Langmuir* **9**:2404 (1993).
23. O. S. Heavens in *Optical Properties of Thin Films* (Butterworths, London, 1955).
24. J. Penfold, in *Neutron, X-ray and Light Scattering*, P. Lindner and T. Zemb, eds. (Elsevier, New York, 1991).
25. T. L. Crowley, E. M. Lee, E. A. Simister, and R. K. Thomas, *Physica B* **173**:143 (1991).
26. J. R. Lu, E. M. Lee, R. K. Thomas, J. Penfold, and S. L. Flitsch, *Langmuir* **9**:1352 (1995).
27. D. G. Bucknall, J. Penfold, J. R. P. Webster, A. Zarbakhsh, R. M. Richardson, A. R. Rennie, J. S. Higgins, R. A. L. Jones, P. D. I. Fletcher, S. Roser, and E. Dickinson, *Proceedings of ICANS-XIII*, PSI Proceedings 95-02 (1995), p. 123.
28. J. Penfold, E. Staples, I. Tucker, and G. Fragnetto, *Physica B* **221**:325 (1996).
29. J. Penfold, E. Staples, I. Tucker, and L. J. Thompson, *Langmuir* **13**:6634 (1998).
30. P. G. Cummins, E. J. Staples, and J. Penfold, *J. Phys. Chem.* **94**:3740 (1990).
31. P. G. Cummins, E. J. Staples, and J. Penfold, *J. Phys. Chem.* **96**:8092 (1990).
32. R. K. Iler, *The Chemistry of Silica* (Wiley–Interscience, New York, 1979).
33. P. M. Holland, *Colloids Surf.* **19**:171 (1986).